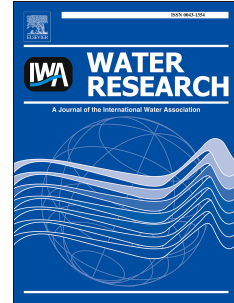# Accepted Manuscript

The role of zeta potential in the adhesion of *E. coli* to suspended intertidal sediments

Adam Wyness, David M. Paterson, Emma Defew, Marc Stutter, Lisa Avery

1 Title

2 The role of zeta potential in the adhesion of *E. coli* to suspended intertidal sediments

3 **Authors**

4 Adam Wyness[a,b], David M. Paterson[a], Emma Defew[a], Marc Stutter[b], Lisa Avery[b]

5 [a] Sediment Ecology Research Group; Scottish Oceans Institute, School of Biology, University of St

6 Andrews, East Sands, St. Andrews, Fife, KY16 8LB, UK.

7 [b] Environmental and Biological Sciences Group; The James Hutton Institute, Craigiebuckler,

8 Aberdeen, UK.

9 Running Title: *E.coli* adhesion to intertidal sediments

10 Abstract

11 The extent of pathogen transport to and within aquatic systems depends heavily on whether the

12 bacterial cells are freely suspended or in association with suspended particles. The surface charge of

13 both bacterial cells and suspended particles affects cell-particle adhesion and subsequent transport

14 and exposure pathways through settling and resuspension cycles. This study investigated the

15 adhesion of Faecal Indicator Organisms (FIOs) to natural suspended intertidal sediments over the

16 salinity gradient encountered at the transition zone from freshwater to marine environments.

17 Phenotypic characteristics of three *E. coli* strains, and the zeta potential (surface charge) of the *E.*

18 *coli* strains and 3 physically different types of intertidal sediments was measured over a salinity

19 gradient from 0 − 5 Practical Salinity Units (PSU). A batch adhesion microcosm experiment was

20 constructed with each combination of *E. coli* strain, intertidal sediment and 0, 2, 3.5 and 5 PSU. The

21 zeta potential profile of one *E. coli* strain had a low negative charge and did not change in response

22 to an increase in salinity, and the remaining *E. coli* strains and the sediments exhibited a more

23 negative charge that decreased with an increase in salinity. Strain type was the most important

24 factor in explaining cell-particle adhesion, however adhesion was also dependant on sediment type

25 and salinity (2, 3.5 PSU > 0, 5 PSU). Contrary to traditional colloidal (Derjaguin, Landau, Vervey, and

26 Overbeek (DLVO)) theory, zeta potential of strain or sediment did not correlate with cell-particle

27 adhesion. *E. coli* strain characteristics were the defining factor in cell-particle adhesion, implying that

28 diverse strain-specific transport and exposure pathways may exist. Further research applying these

29 findings on a catchment scale is necessary to elucidate these pathways in order to improve accuracy

30 of FIO fate and transport models.

31 **Keywords:** Pathogen, Adhesion, DLVO Theory, Zeta potential, Intertidal sediment

32 # 1. Introduction

33 In the early 2000s, it was predicted that local and foreign tourists spent two billion days each year at

34 the coast worldwide (Shuval 2003), and an estimated 20 million people used the coast and inland

35 waters each year in the UK (Pond 2005), with these numbers predicted to increase. Around this

36 period, bathing at coastal sites caused an estimated 120 million cases of gastrointestinal illness

37 worldwide (Shuval 2003), and bathing at English and Welsh beaches and bathing waters caused an

38 estimated 1.75 million cases of gastrointestinal disease annually (Georgiou and Langford 2002). The

39 most common disease associated with bathing in contaminated water is enteric illness with an

40 associated risk of roughly 51/1000 bathers, and the risk of other respiratory, ear and eye disease

41 between 20/1000 and 54/1000 bathers in water that contained <2000 faecal coliforms 100 ml^{-1}

42 (Fleisher et al. 1998). The likelihood of gastrointestinal illness to sea-bathers compared to non-

43 bathing beach goers increases 1.76 fold (Fleisher et al. 2010). However, risk is not solely associated

44 with bathers, as an increase in enteric illnesses can be a direct result from increased contact with

45 recreational beach sand (Heaney et al. 2012).

46   It is well established that survival of FIOs is greatly increased when in association with sediments

47   compared to the overlying water in both freshwater and marine systems (Gerba and Mcleod 1976;

48   Moore et al. 2003; Pachepsky and Shelton 2011). This is a result of many survival advantages

49   including increased nutrient availability (Burton et al. 1987) and protection from UV (Fujioka and

50   Yoneyama 2002) and protozoan grazing (England et al. 1993). Faecal Indicator Organisms gain these

51   survival advantages through adhering to particles in suspension, leading to incorporation of FIOs in

52   sediments as the particle is deposited (Davies et al. 1995; Geldreich 1970).

53   The transport and fate, and therefore spatial and temporal abundance, of faecal indicator organisms

54   (FIOs) within aquatic systems is heavily dependent on whether cells are freely suspended, or

55   associated with suspended particles (Bai and Lung 2005; Jeng et al. 2005; Muirhead et al. 2006b).

56   Particle association also governs FIO residence time through incorporation into the erosion,

57   transport, deposition and consolidation (ETDC cycle) of particles (Whitehouse 2000). The importance

58   of differentiating between these phases has been realised in recent modelling approaches

59   concerning FIO fate and transport on catchment scales (Cho et al. 2016b).

60   Free bacterial cells in the water column are maintained in suspension by Brownian motion but

61   become susceptible to sedimentation when in association with particles because of the increased

62   settling velocity. The mechanisms governing the adhesion of faecal bacteria to suspended particles

63   are complex and may be determined by a range of physical, and biological factors (Oliver et al.

64   2007). Derjaguin, Landau, Vervey, and Overbeek (DLVO) theory is known to serve as a basic model

65   for describing the initial adhesion of bacteria to suspended particles (Van Loosdrecht et al. 1990),

66   and has been since been improved upon for the prediction of cell adhesion with the extended DLVO

67   theory (xDLVO) (Perni et al. 2014)

68   Briefly, DLVO theory describes the interplay between electrostatic repulsion and the attraction of

69   Van der Waals forces between colloidal particles. The strength of the electrostatic repulsion can be

70   determined by measuring the particle charge, known as the zeta potential, of a colloidal suspension.

71 As zeta potential becomes more positive or negative, the larger the electrostatic repulsion between

72 particles, the less likely they are to flocculate (Van Loosdrecht et al. 1987).

73 In this study, phenotyping assays and zeta potential analyses were followed by a microcosm

74 experiment using natural intertidal sediments and river and seawater in order to investigate the role

75 of strain and sediment characteristics and particle charge in the adhesion of *E. coli* to suspended

76 particles. It was hypothesised that the less negative zeta potentials of cell and/or sediments induced

77 by higher salinity would correlate with increased cell- particle adhesion.

78

2. Materials and Methods

79

2.1 *E. coli* strains

80

81 One of several wild-type *E. coli* strains isolated from intertidal sediment at the Ythan estuary,

82 Scotland, UK (57°20'59.3" N 1°59'36.8" W) in May 2014 was selected for use and hereby referred to

83 as Yth13 throughout. *E. coli* strains DSM 8698 and DSM 9034 were obtained from the Leibniz

84 Institute DSMZ (Germany). Serological and isolation details are provided in Table 1.   Unless

85 otherwise stated, *E. coli* cultures were prepared from -80 °C stock cultures through overnight

86 incubation in LB broth at 37 °C in a shaking incubator at 150 rpm. Cells were harvested by

87 centrifugation at 3000 x g for 5 minutes, and washed three times in the appropriate dilution of

88 seawater.

2.2 Bacterial strain characterisation

89

90 Swarm assays were performed using a similar method to that of Wolfe and Berg (1989). Cells from a

91 single colony were stab-inoculated into the centre of a 0.4 % LB agar plates (LB broth, Merck

92 Millipore, Darmstadt, Germany). Three replicate plates for each strain at each temperature

93 treatment (15 ˚C and 25 ˚C) were sealed with laboratory film to reduce moisture loss, inverted and

94 incubated. The swarm diameter was measured to the nearest mm every 24 hours.

4

95   Biofilm assays were performed using a similar method to that of Merritt et al. (2011). Briefly, *E. coli*

96   cultures were grown overnight in 5 ml LB broth at 37 ˚C. Cultures were normalised to an OD600 of

97   0.5 using 70-850 µl disposable micro-cuvettes (Brand GMBH + CO KG, Germany) in a

98   spectrophotometer (BioPhotometer 6131, Eppendorf). One µl of each normalised *E. coli* culture was

99   inoculated into 4 replicate wells in a sterile 96 well cell culture plate (Costar, Corning, NY, USA)

100   alongside 4 wells containing media only controls. One hundred µl of fresh sterile LB broth media was

101   added to each well. The plate was covered with laboratory film to minimise evaporation and

102   incubated at 25 °C for 48 hours. After incubation, the plate was washed twice with DI H_2O, and 125 µl

103   of 0.1% (w/v) crystal violet in DI H_2O was added to each well and the plate incubated for 10 minutes

104   at room temperature. The plate was rinsed as above and left to air dry before 200 µl of 80:20

105   ethanol: acetone solution (O'Toole et al. 1999) was added to each well and the plate incubated for

106   15 minutes at room temperature. The contents of each well were mixed via pipetting, and 125 µl

107   transferred to a micro-cuvette with the OD600 of each biofilm elution measured against a blank of

108   the ethanol: acetone solution.

109

110 2.3 Sediment and Water Properties

111   Intertidal sediments with differing properties (Mud (M), Organic Mud (OM) and Mixed Sand (MS))

112   were collected from 3 locations within the Ythan estuary, Scotland, UK (Table 2). Bulk sediment for

113   the microcosms was collected from the surface to 10 mm depth. Cores to a depth of 10 mm with a

114   volume of 3.14 cm^3 were taken for measurement of bulk density. Sediments were dried at 105 ˚C for

115   24 hours, then ignited in a furnace at 450 ˚C for 12 hours to determine water content and organic

116   content respectively. Laser particle size distribution was analysed using a Malvern Mastersizer 2000

117   (Malvern Instruments Ltd., UK). Sediment surface area was measured by adsorption of nitrogen gas

118   (Coulter SA 3100, Beckmann Coulter, UK) and calculated using the Brunauer, Emmett and Teller

119   equation (Brunauer et al. 1938) using 10 points in the analysis. X-Ray Powder Diffraction (XRPD)

120　analysis was performed to determine sediment bulk mineralogy. Briefly, freeze-dried samples were

121　hand ground, then wet milled in ethanol (McCrone Mill, McCrone, IL, USA) and spray dried. XRPD

122　patterns were recorded from 3-70°2θ using Copper Kα radiation with a Panalytical Xpert Pro

123　diffractometer equipped with an Xcelerator detector.

124　River water was collected from the River Ythan beyond the tidal range (57°21'48.5"N 2°04'23.9"W),

125　and　sea water collected from Collieston Harbour located 5 km Northeast of the estuary mouth

126　(57°20'50.4"N 1°56'03.6"W). Soluble elemental analysis was performed using standard procedures

127　on a Skalar SAN^{++} autoanalyser (Skalar Analytical B. V., Netherlands).

128

2.4 Microcosm preparation

130　River water (0.11 PSU) and sea water (34.5 PSU) were vacuum filtered through 0.45 µm filter paper

131　(Merck Millipore, MA, USA). Solutions of river water (hereby referred to as 0 PSU), 1, 1.5, 2, 2.5, 3,

132　3.5, 4 and 5 PSU were created by mixing the stock waters whilst monitoring the salinity change.

133　Salinity and pH were recorded at using a Hach HQ40d multi-probe (Hach Lange, UK). The equivalent

134　of 50 g dry weight of each sediment type was weighed into 700 ml centrifuge vessels, suspended in

135　250 ml DI H$_2$O and centrifuged at 1450 x g for 15 minutes. The supernatant was removed, and the

136　washing procedure repeated twice. Sediment was finally resuspended in 500 ml (1 g sediment: 10 ml

137　water) of the appropriate salinity solution. Sediment suspensions were then sonicated for 5 minutes

138　at 20 % power with the microtip attachment (600 W Ultrasonic Processor, Sonics and Materials Inc.,

139　CT, USA). The sediment was kept in suspension by magnetic stirring, and 20 ml suspension aliquoted

140　into 3 replicate 50 ml falcon tubes for each *E. coli* strain/ salinity suspension. Overnight cultures of *E.*

141　*coli* strains Yth13, DSM 8698 and DSM 9034 prepared as in Section 2.1 and inoculated into

142　microcosms at a final inoculum concentration of 1 x 10^7 CFU ml^{-1}. Additional non-inoculated controls

143　and non-sediment microcosms were prepared. Microcosms were incubated at 12 ˚C for 90 minutes,

144　with a shaking speed of 300 rpm in order to keep sediment particles in suspension.

6

145

2.5 Quantification of adhered *E. coli*

147 Post-incubation, microcosms were centrifuged at 500 x *g* for 120 s at 12 ˚C to separate non-adhered

148 *E. coli* from those adhered to particles > ~1.55 μm according to Stokes' law. Triplicate aliquots of 20

149 μl of supernatant were removed at a depth of 15 mm and serial dilutions made to 10^{-8}. Twenty μl of

150 each serial dilution was pipetted from 10 mm onto HiCrome Coliform agar plates (Sigma Aldrich, UK)

151 and, when dry, the plates inverted and incubated at 37 ˚C for 18 hours. Non-inoculated microcosms

152 were analysed in order to enumerate *E. coli* pre-existing in each sediment. The inoculum culture and

153 non-sediment microcosms were also analysed to establish the recovery of viable *E. coli* after the

154 centrifugation and quantification process. Recovered *E. coli* values were normalised to an inoculum

155 density of 1 x 10^7 CFU ml $^{-1}$. Non- recovered *E. coli* (non- sediment control microcosms) were added

156 to the resulting value, and this subtracted from the inoculum density to give a final concentration of

157 adhered *E. coli*.

158

2.6 Zeta potential measurements

160 Zeta potential measurements were made on *E. coli* cultures prepared as for microcosm inoculation,

161 and non-inoculated sediment microcosms were left to settle for 15 minutes to reduce particle

162 settling during the measurement. Measurements were performed using the Zetasizer Nano ZS

163 (Malvern Instruments, UK) using the DTS 1070 cell at 12 ˚C using fresh samples for each of three

164 replicates. In order to avoid electrode and sample degradation at the higher salinities (Malvern

165 2014), automatic voltage selection, monomodal analysis only, and a 60 s delay between

166 measurements were applied. Zeta potential was calculated from the electrophoretic mobility of

167 particles using the Smoluchowski model (Hiemenz 1977) with a fixed F(ka) value of 1.5.

168 ## 2.7 Statistical analyses

169 Mean absorbance of the media-only controls in the biofilm assay was subtracted from each sample

170 absorbance. Data was square root transformed to comply with the assumptions of ANOVA.

171 Comparison of swarm diameter means at each time point was performed using ANOVA after

172 Bonferroni correction of the family-wise significance threshold to p = 0.0026 to account for multiple

173 comparisons. Zeta potential measurements were analysed using two-way ANOVA with salinity and

174 either strain or sediment type as factors.

175 Any *E. coli* enumerated from the non-inoculated microcosms were subtracted from the counts from

176 the relevant inoculated microcosms. Recovered *E. coli* counts from the microcosms were normalised

177 to the same inoculum concentration adjusted according to non-recovered CFUs obtained from the

178 non-sediment controls. Counts were then log transformed to meet the assumptions of ANOVA to

179 produce the amount of $\log_{10}$ sediment-adhered *E. coli* CFU ml^{-1}. All statistics were performed using

180 Genstat (GenStat Release 18.1 (PC/Windows); VSN International Ltd., 2015), and figures created

181 using SigmaPlot (SigmaPlot 13.0, Systat Software Inc., CA, USA).

182

183

184 # 3. Results

185 ## 3.1 Bacterial strain characteristics

186 There were large differences between the phenotypic characteristics of the three *E. coli* strains. The

187 absorbance in the biofilm assay for DSM 8698 was over 4 times greater than the wild-type strain

188 Yth13 (One-way ANOVA; F- statistic of strain effect= 30.093, total d.f.= 11, p < 0.001), which in turn

189 was almost 4 times greater than DSM 9034 (p < 0.001) (Table 3). Growth rates of swarm colonies

190 rates were higher for all strains at 25 ˚C than 15 ˚C (Table 3). At 15 ˚C the swarm colony diameter of

191 DSM 9034 was significantly smaller than other strains from Day 3 (One-way ANOVA; F- statistic of

8

192 strain effect= 61.00, total d.f.= 8, $p < 0.001$), and Yth13 became significantly larger than DSM 8698

193 from Day 5 ((One-way ANOVA; F- statistic of strain effect= 127.00, total d.f.= 8, $p < 0.001$). At 25 ˚C

194 all replicates of DSM 8698 had reached the edge of the petri dish (85 mm) within 3 days, whereas

195 DSM 9034 and Yth13 demonstrated a more moderate increase in swarming rate compared to 15 ˚C

196 with the size of DSM 9034 significantly smaller than Yth13 again from Day 3 (One-way ANOVA; F-

197 statistic of strain effect= 25908.50, total d.f.= 8, $p < 0.001$).

198 The two-way interaction of strain and matrix salinity influenced the zeta potential of *E. coli* strains

199 (Two- way ANOVA; F- statistic of strain x sediment interaction= 18.044; total d.f.= 80; $p < 0.001$). The

200 zeta potential of DSM 9034 was much less negative than the other strains and changed minimally

201 across the salinity gradient (mean -3.23 ± SE 0.07 mV). DSM 8698 and Yth13 followed a similar trend,

202 remaining relatively stable at around -23 and -19 mV respectively between 0 and 2.5 PSU where

203 thereafter they became increasingly less negative with increasing matrix salinity before starting to

204 plateau between 4 and 5 PSU, following a sigmoidal trend with a point of inflection at roughly 3 PSU

205 (Fig. 1).

206

3.2 Sediment and water characteristics

208 Organic Mud (OM) and Mud (M) sediments had similar physical characteristics, whereas the Mixed

209 Sand (MS) had a higher bulk density, lower surface area, lower water and organic content and more

210 coarse particles (Table 2 and Supplementary Table 1). Mud had a slightly higher bulk density and

211 lower water and organic content than OM. X-Ray Powder Diffraction (XRPD) bulk mineralogy analysis

212 indicated a broadly similar abundance of minerals across all sediments, except MS contained a much

213 greater quartz content (Supplementary Table 2). Organic Mud also contained larger fractions of the

214 clay minerals kaolinite, trioctahedral clays and illite/muscovite, and smaller fractions of the

215 carbonate minerals aragonite and calcite than M. The river water collected beyond the tidal range

216 contained a lower NH_4 concentration than the sea water, but had a higher concentration of all other

217   components analysed (Supplementary Table 3). The chemistry of the river water used in this

218   experiment was in line with the average levels for the Ythan river as reported by SEPA (SEPA 2013).

219   Sediment zeta potential generally became slightly less negative as matrix salinity increased (One-way

220   ANOVA; F- statistic of salinity effect= 104.99; total d.f.= 35) (Fig. 2), with the magnitude of change

221   less than *E. coli* strains DSM 8698 and Yth13. The mean zeta potential for all sediments was more

222   negative at 2 PSU and below than 3.5 PSU and above ($p < 0.001$; 0 PSU: mean -21.38 ± SE 0.35 mV, 2

223   PSU: -20.83 ± 0.03 mV, 3.5 PSU: -17.03 ± 0.09 mV, 5 PSU: -16.11 ± 0.08 mV). The mean zeta potential

224   over all salinities also differed with sediment type, where OM was less negative than M and MS

225   sediments ($p < 0.001$; OM: -17.30 ± 0.05 mV, M: -19.30 ± 0.10 mV, MS: -19.91 ± 0.28 mV).

226

3.3 Adhesion of *E. coli* to sediments

228   There was no significant difference between *E. coli* numbers recovered from the different strain and

229   salinity treatments of non-sediment control microcosms indicating negligible treatment effects, cell-

230   cell adhesion or die-off during the incubation or centrifugation process.

231   *E. coli* adhesion to sediment particles increased with sediment type in the order OM > M > MS over

232   all salinities and sediment types, however, only the difference between OM and MS was statistically

233   significant (One-way ANOVA; F- statistic of sediment effect= 5.34, total d.f. 108; $p = 0.007$; Table 4).

234   Adhesion of *E. coli* cells was significantly greater with strain DSM 8698 than both Yth13 and DSM

235   9034 (One-way ANOVA; F- statistic of strain effect= 43.38, total d.f. 108; $p < 0.001$). The adhesion of

236   *E. coli* cells was significantly greater at 2 and 3.5 PSU than 0 and 5 PSU ($p < 0.001$).

237   DSM 8698 exhibited the greatest adhesion of all strains to M (Two-way ANOVA; F- statistic of

238   sediment x strain effect= 25.28, total d.f. 108; $p < 0.001$) (Table 5; Fig. 3B). DSM 9034 adhered the

239   least to M and demonstrated no major changes with salinity within treatments. In contrast, adhesion

240   of DSM 8698 peaked at 2 PSU, and Yth13 peaked at 3.5 PSU to M. In OM and MS, these peaks of

10

241   adhesion for DSM 8698 and Yth13 were evident at the same salinities, and up to 2-fold higher than

242   other salinities (Table 5, Fig. 3). With the exception of these peaks, in OM the strains exhibited

243   broadly similar levels of adhesion across the salinity gradient (Fig. 3A). In MS, Yth13 adhered less

244   than it did to other sediments, and to other strains to MS (Table 5, Fig. 3C).

245   Increase in zeta potential of the sediments significantly correlated with decreasing pH of sediment

246   suspension as salinity increased. despite the narrow range of pH values observed (7.60 – 7.96) (n=

247   12, Adjusted R^2= 0.66, *p* < 0.001). However there was no significant relationship between sediment

248   zeta potential and the number of adhered *E. coli.* Strain zeta potential explained little of the

249   variation in adhesion of *E. coli* despite a significant relationship (n= 108, Adjusted R^2=0.09, *p* <

250   0.001).

251

252

253

254   4. Discussion

255   The zeta potential of all *E. coli* suspensions were negative, which is widely recognised to be the case

256   for bacteria in natural aquatic systems (Rijnaarts et al. 1995; Sokolov et al. 2001; Van der Wal et al.

257   1997; Walker et al. 2004). The zeta potential profiles of *E. coli* strains in this study formed two

258   distinct profile shapes; the stable profile of DSM 9034, and the sigmoidal curve of Yth13 and DSM

259   8698 with less negative zeta potential as ionic strength increased. The sigmoidal profile has been

260   previously observed with different *E. coli* strains in increasing concentrations of NaCl and KCl (Chen

261   and Walker 2012; Zhao et al. 2014). The decrease in zeta potential with increasing ionic strength is

262   consistent with classic DLVO theory, resulting from charge screening by counter ions and increasing

263   electrostatic double-layer compression (Kim et al. 2010; Walker et al. 2004). The limit of the

264   decrease in zeta potential and subsequent plateau at higher electrolyte concentrations is explained

11

265 by a limit on the compression of the double layer of counterions surrounding the particle (Sharma et

266 al. 1985). Instability of zeta potential similar to that exhibited by strains Yth13 and DSM 8698

267 between 0 and 2 PSU was previously observed in *E. coli* in low (10- 20 mM) concentrations of

268 phosphate buffer (Carlsson 2012). The difference in the zeta potential profiles in this study are likely

269 to be the result of differing cell surface morphology and lipopolysaccharide structures (Walker et al.

270 2004) and flagellar, fimbrae and curlin proteins, all of which are known to affect zeta potential (Feng

271 et al. 2014).

272 Sediment zeta potential became less negative with increasing salinity and followed the same

273 sigmoidal curve as the Yth13 and DSM 8698 *E. coli* strains. However, the magnitude of change was

274 less for sediments than that of the *E. coli* strains, an observation made previously by Zhao et al

275 (2014) who proposed it to be a result of the combination of variably and permanently charged

276 minerals and organic matter present in soil colloids compared to pure samples. Similar sigmoidal

277 trends have been observed for soil colloids at similar electrolyte concentrations with a plateau at 50

278 mM of KCl solution (~3.5 PSU) (Zhao et al. 2014), and for suspended estuarine particles with a

279 plateau at 5- 7.5 PSU seawater (Hunter and Liss 1982). The zeta potential profiles are similar

280 between sediment types despite the physical and mineralogical differences. This may be attributed

281 to organic conditioning films, chiefly proteinaceous substances that cover particle surfaces and are

282 found especially in highly productive environments such as estuaries, that can neutralise any

283 physico-chemical features of the surface, including surface charge (Donlan 2001).

284 Despite large and significant differences in the zeta potentials of different bacterial strains and

285 sediments over the salinity gradient, there was no significant correlation between zeta potential and

286 adhesion of cells to suspended sediments. Visual inspection revealed decreased turbidity with

287 increased salinity in microcosms post-centrifugation due to increased particle-particle adhesion and

288 flocculation of sediment particles at higher salinities in line with DLVO theory) identified a critical

289 salinity equivalent to ~1.22 PSU, below which *E. coli* cells became desorbed from a mixed sediment,

290   therefore it may be that adhesion between 0 and 3.5 PSU is in accordance with classic DLVO theory,

291   but this was inhibited or superseded at 5 PSU by stronger metabolic or physiological factors.

292   Increased salinity is well known to cause sub-lethal and lethal stress in *E. coli* (Anderson et al. 1979;

293   Carlucci and Pramer 1960), with *E. coli* growth rates observed to peak at intermediate

294   concentrations of NaCl and KCl (Abdulkarim et al. 2009), and seawater (Carlucci and Pramer 1960).

295   The metabolic response of *E. coli* to saline stress is complex, involving the accumulation of K^+ ions

296   and several osmosprotective and membrane-stabilizing endogenously synthesized organic solutes

297   (Sevin et al. 2016). Despite the relatively high saline tolerance of *E. coli* (Sevin et al. 2016), at the

298   higher osmotic stress of 5 PSU activation of stress response factors leading to alteration of cell wall

299   characteristics may be resulting in decreased adhesion to particles.

300   Trends in particle-cell adhesion observed here did not strictly follow DLVO theory, which supports

301   the conclusions of Rong et al. (2008) that non-electrostatic mechanisms rather than electrostatic

302   forces are more important in bacterial adhesion to particles. In the systems studied, it is postulated

303   that the turbulence simulated in the microcosms exceeded or obscured any electrostatic

304   interactions. Therefore, cell characteristics such as adhesins, fimbrae and flagella became more

305   significant than particle charge in successful adhesion under turbulence-mediated cell-particle

306   collisions. Future investigations into how cell surface morphology and characteristics effect adhesion

307   in natural systems are necessary in order to elucidate the mechanisms at work."

308   *E. coli* adhered better to sediments with larger proportions of fine particles (DSM 8698- M, Yth13-

309   OM, DSM 9034- MS, OM). This preferential adhesion by different strains has been observed by

310   Pachepsky et al. (2008) where the authors found 80 % of strains adhering to silt particles were not

311   found adhered to fine sand, with further strains found only to adhere to sands and not to silt or clay.

312   Similarly, several studies have observed greater adhesion of *E. coli* to soil particles of smaller size

313   fractions. However, Oliver et al. (2007) observed that although the greatest number of *E. coli* bound

314   to the 4-15 μm fraction of suspended soil particles, the 16-30 μm fraction had almost 4 times the

13

315   amount of adhered *E. coli* after adjustment for surface area. Muirhead et al. (2006) also found most

316   *E. coli* was being transported in overland flow in association with soil particles in the <20 μm

317   fraction.

318   The strains examined here exhibited very different phenotypic characteristics, however there was no

319   obvious correlation or trend between these and adhesion success despite strain type remaining the

320   most important factor determining adhesion extent. It has been established that there is strain

321   dependant preference of adhesion to suspended soils and sediments (Oliver et al. 2007; Pachepsky

322   et al. 2008), however the work presented here demonstrates that this preference is dependant on

323   sediment type and salinity. This is further complicated by the variation in the persistence between

324   strains that has been observed in freshwater microcosms (Anderson et al. 2005) and between soil

325   types (Ma et al. 2014).

326   Therefore the spatial variation in the abundance of strains of a single species in intertidal sediments

327   depends on strain input, salinity and suspended sediment characteristics. The highest adhesion of E.

328   coli to sediment particles was observed in this study at 2- 3.5 PSU. These salinities would be

329   encountered by FIOs being transported down-catchment at the tidal limits of estuaries and where

330   freshwater tributaries enter the estuary. Due to the dynamic hydrological regimes of estuaries, the

331   location of this transitional zone will vary spatially and temporally. Environmental conditions will

332   also affect where and when conditions allowing for increased adhesion will occur. For example,

333   increased rainfall increases FIO transport from land to surface waters (Guber et al. 2006; Muirhead

334   et al. 2004; Oliver et al. 2005) and will also push the tidal limit, where fresh and sea water mix,

335   further down the river channel resulting in higher adhesion and deposition of certain strains lower

336   down the estuary.

337   The variability in *E. coli* adhesion presented here introduces complications for catchment models of

338   FIO fate and transport that concern sediment-water exchange and sediment-fate of FIOs to

339   accurately predict disease risk. Firstly, it highlights the possible ecological discrepancies between

340   pathogen and non-pathogen strains of bacteria. The difference in adhesion of the different strains

341   observed here are attributed to physiological differences independent of particle charge. Many

342   physiological adaptations of pathogenic strains may be advantageous to cell-particle adhesion

343   therefore there may be bias to how pathogen and non-pathogen strains are distributed in the

344   environment. This is especially potent considering emerging evidence that sediments contribute a

345   more significant proportion of FIOs to surface waters than previously thought through hyporheic

346   exchange (Pachepsky et al. 2017). Since the use of FIOs such as *E. coli* are based upon correlation

347   between total FIO loading and risk of disease, further work must be undertaken on a catchment

348   scale to elucidate this relationship in order predict where pathogenic strains may be occurring in

349   relatively high abundance to total FIOs. Secondly it is demonstrated here that, in addition to the

350   known effects of salinity in faecal bacteria die-off that have been incorporated into recent FIO fate

351   and transport models (Gao et al. 2015), salinity should also be considered in sediment-bacteria

352   interaction sub models such as that of Gao et al. 2011. Finally, this study furthers the understanding

353   of *E. coli* preference to sediment types as discussed above. This is especially important to recent

354   modelling efforts that incorporate sediment-water column exchange of FIOs (Cho et al. 2016a; Feng

355   et al. 2015).

356   It was hypothesised that where the zeta potential of cell or sediment suspension was less negative,

357   the more cell-particle adhesion would occur. Adhesion instead varied greatly between strain type

358   independent of zeta potential, was higher at 2 and 3.5 PSU than 0 and 5 PSU, and was slightly higher

359   with smaller particle sediments with large surface area and high organic matter.

360

361   **Conclusions**

362   •   *This study highlights the multiple drivers of cell-particle adhesion and its importance in*

363   *respect to bacterial transport and fate.*

364   •   *Despite large shifts in zeta potential for both cell and particle suspensions within the narrow*

365   *range of salinities typical of the upper reaches of an estuary, zeta potential was a poor*

366   *indicator of particle adhesion potential and therefore should be used with caution to inform*

367   *upon bacterial transport pathways.*

368   •   *Bacterial strain type was the most important factor in adhesion, highlighting the importance*

369   *of understanding cell characteristics of pathogens in the environment.*

370   •   E. coli *are likely to adhere to suspended sediments and subsequently be deposited at the tidal*

371   *limit of estuaries where salinities of around 2- 3.5 PSU are encountered, and where*

372   *sediments with small particle sizes and high organic matter are found.*

373

374 **Acknowledgments**

378

379

380

381

382 **Figure Legends**

383 **Table 1.** Summary information of the *E. coli* strains used in this study including clade (Clermont et al.

384 2013) and MLST Complex (Wirth et al. 2006). DSMZ refers to the Leibniz Institute Deutsche

385 Sammlung von Mikroorganismen und Zellkulturen.

386 **Table 2.** Summary of bulk sediment characteristics for the 3 sediment types used.

387   **Table 3.** Extent of biofilm formation (n=4) and swarm diameter (n=3) for *E. coli* strains.

388   **Table 4.** General ANOVA summary table. F- statistics and *p*- values are for single factor effects.

389   Significantly different groups identified using Fisher's LSD test and are displayed in brackets under

390   the *p*-value.

391   **Table 5.** Summary of E. coli adhesion ($\log_{10}$ CFU ml^{-1} ± SE) for treatment interactions (n= 3).

392   **Figure 1.** Zeta potential measurements of cell suspensions of Yth13, DSM 8698 and DSM 9034 over a

393   salinity gradient (0- 5 PSU). Hollow circles- Yth13; solid triangles- DSM 8698; hollow triangles- DSM

394   9034. Error bars indicate SE (n= 3).

395   **Figure 2.** Zeta potential measurements of Organic Mud, Mud, Mixed Sand sediments at 0, 2, 3.5 and

396   5 PSU. Solid circles- Organic Mud; hollow circles- Mud; solid triangles- Mixed Sand. Error bars

397   indicate SE (n= 3).

398   **Figure 3.** Number of adhered *E. coli* CFUs to sediment particles (bars) and zeta potential

399   measurements of the sediment (solid circles) and 0, 2, 3.5 and 5 PSU. A- Organic Mud; B- Mud; C-

400   Mixed Sand. Solid fill bars- Yth13; dashed bars- DSM 8698; hatched bars- DSM 9034. Error bars

401   indicate SE (n= 3).

402   **Supplementary Table 1.** Particle size distribution of the Organic Mud (OM), Mud (M) and Mixed

403   Sand (MS) sediments. Modelled diameter parameters

404   **Supplementary Table 2.** Bulk mineralogical analysis of the Organic Mud (OM), Mud (M) and Mixed

405   Sand (MS) sediments.

406   **Supplementary Table 3.** Sampling location and water chemistry of the collected Ythan river water

407   and seawater.

408

17

409

410

411

412

References

414 Abdulkarim SM, Fatimah AB, Anderson JG (2009) Effect of salt concentrations on the growth of heat-
415   stressed and unstressed *Escherichia coli*. Food, Agriculture and Environment 7(3&4):51-54

416 Anderson IC, Rhodes M, Kator H (1979) Sublethal stress in *Escherichia coli*: a function of salinity.
417   Applied and environmental microbiology 38(6):1147-1152

418 Anderson KL, Whitlock JE, Harwood VJ (2005) Persistence and differential survival of fecal indicator
419   bacteria in subtropical waters and sediments. Applied and environmental microbiology
420   71(6):3041-3048 doi:10.1128/aem.71.6.3041-3048.2005

421 Bai S, Lung WS (2005) Modeling sediment impact on the transport of fecal bacteria. Water Research
422   39(20):5232-40 doi:10.1016/j.watres.2005.10.013

423 Brunauer S, Emmett PH, Teller E (1938) Adsorption of gases in multimolecular layers. Journal of the
424   American Chemical Society 60(2):309-319 doi:10.1021/ja01269a023

425 Burton GA, Gunnison D, Lanza GR (1987) Survival of pathogenic bacteria in various freshwater
426   sediments. Applied and environmental microbiology 53(4):633- 638

427 Carlsson S (2012) Surface characterization of gram-negative bacteria and their vesicles. Thesis in
428   Chemistry, Umeå University

429 Carlucci AF, Pramer D (1960) An evaluation of factors affecting the survival of *Escherichia coli* in sea
430   water: II. Salinity, pH, and nutrients. Applied Microbiology 8(4):247-250

431 Chen G, Walker SL (2012) Fecal indicator bacteria transport and deposition in saturated and
432   unsaturated porous media. Environmental Science and Technology 46(16):8782-90
433   doi:10.1021/es301378q

434 Cho KH, Pachepsky YA, Kim M, Pyo J, Park M-H, Kim YM, Kim J-W, Kim JH (2016a) Modeling seasonal
435   variability of fecal coliform in natural surface waters using the modified SWAT. Journal of
436   Hydrology 535:377-385 doi:http://dx.doi.org/10.1016/j.jhydrol.2016.01.084

437 Cho KH, Pachepsky YA, Oliver DM, Muirhead RW, Park Y, Quilliam RS, Shelton DR (2016b) Modeling
438   fate and transport of fecally-derived microorganisms at the watershed scale: State of the
439   science and future opportunities. Water Research 100:38-56
440   doi:https://doi.org/10.1016/j.watres.2016.04.064

441 Clermont O, Christenson JK, Denamur E, Gordon DM (2013) The Clermont *Escherichia coli* phylo-
442   typing method revisited: improvement of specificity and detection of new phylo-groups.
443   Environmental Microbiology Reports 5(1):58-65 doi:10.1111/1758-2229.12019

444 Davies CM, Long JAH, Donald M, Ashbolt NJ (1995) Survival of fecal microorganisms in marine and
445   freshwater sediments. Applied and environmental microbiology 61(5):1888- 1896

446 Donlan RM (2001) Biofilm formation: A clinically relevant microbiological process. Clinical Infectious
447   Diseases 33(8):1387-1392 doi:10.1086/322972

448 England LS, Lee H, Trevors JT (1993) Bacterial survival in soil: effect of clays and protozoa. Soil
449   Biology and Biochemistry 25(5):525-531

450 Feng G, Cheng Y, Wang S-Y, Hsu LC, Feliz Y, Borca- Tasciuc DA, Worobo RW, Moraru CI (2014)
451   Alumina surfaces with nanoscale topography reduce attachment and biofilm formation by
452   *Escherichia coli* and *Listeria* spp. Biofouling 30(10):1253-1268
453 Feng Z, Reniers A, Haus BK, Solo-Gabriele HM, Wang JD, Fleming LE (2015) A predictive model for
454   microbial counts on beaches where intertidal sand is the primary source. Marine Pollution
455   Bulletin 94(0):37-47 doi:10.1016/j.marpolbul.2015.03.019
456 Fleisher JM, Fleming LE, Solo-Gabriele HM, Kish JK, Sinigalliano CD, Plano L, Elmir SM, Wang JD,
457   Withum K, Shibata T, Gidley ML, Abdelzaher A, He G, Ortega C, Zhu X, Wright M, Hollenbeck
458   J, Backer LC (2010) The BEACHES Study: health effects and exposures from non-point source
459   microbial contaminants in subtropical recreational marine waters. International Journal of
460   Epidemiology 39(5):1291-8 doi:10.1093/ije/dyq084
461 Fleisher JM, Kay D, Wyer M, Godree AF (1998) Estimates of the severity of illnesses associated with
462   bathing in marine waters contaminated with domestic sewage. International Journal of
463   Epidemiology 27:722-726
464 Fujioka RS, Yoneyama BS (2002) Sunlight inactivation of human enteric viruses and fecal bacteria.
465   Water Science and Technology 46:291- 295
466 Gao G, Falconer RA, Lin B (2011) Numerical Modelling Sediment-Bacteria Interaction Processes in the
467   Severn   Estuary.   Journal   of   Water   Resource   and   Protection   03(01):22-31
468   doi:10.4236/jwarp.2011.31003
469 Gao G, Falconer RA, Lin B (2015) Modelling the fate and transport of faecal bacteria in estuarine and
470   coastal   waters.   Marine   Pollution   Bulletin   100(1):162-168
471   doi:https://doi.org/10.1016/j.marpolbul.2015.09.011
472 Geldreich EE (1970) APPLYING BACTERIOLOGICAL PARAMETERS TO RECREATIONAL WATER QUALITY.
473   Journal (American Water Works Association) 62(2):113-120
474 Georgiou S, Langford IH (2002) Coastal bathing water quality and human health risks: a review of
475   legislation, policy, and epidemiology, with an assessment of current uk water quality,
476   proposed standards, and disease burden in England and Wales. CSERGE, Working Paper ECM
477   02-06, England
478 Gerba CP, Mcleod JS (1976) Effect of sediments on the survival of *Escherichia coli* in marine waters.
479   Applied and environmental microbiology 32(1):114- 120
480 Guber AK, Shelton D, Pachepsky Y, Sadeghi AM, Sikora LJ (2006) Rainfall-induced release of fecal
481   coliforms   and   other   manure   constituents: comparison   and   modeling.   Applied   and
482   environmental microbiology 72(12):7531- 7539
483 Heaney CD, Sams E, Dufour AP, Brenner KP, Haugland RA, Chern E, Wing S, Marshall S, Love DC,
484   Serre M, Noble R, Wade TJ (2012) Fecal indicators in sand, sand contact, and risk of enteric
485   illness among beachgoers. Epidemiology 23(1):95-106
486 Hiemenz PC (1977) Electrophoresis and other electrokinetic phenomena. In: Lagowski JJ (ed)
487   Principles of Colloid and Surface Chemistry. Marcel Dekker, New York, pp 452-487
488 Hunter KA, Liss PS (1982) Organic matter and the surface charge of suspended particles in estuarine
489   waters Limnology and Oceanography 27(2):322- 335
490 Jeng HAC, Englande AJ, Bakeer RM, Bradford HB (2005) Impact of urban stormwater runoff on
491   estuarine environmental quality. Estuarine, Coastal and Shelf Science 63(4):513-526
492   doi:10.1016/j.ecss.2004.11.024
493 Kauffmann F, Dupont A (1950) *Escherichia* strains from infantile epidemic gastro enteritis. Acta
494   Pathologica Microbiologica Scandinavica 27(4):552-64
495 Kim HN, Walker SL, Bradford SA (2010) Macromolecule mediated transport and retention of
496   Escherichia coli O157:H7 in saturated porous media. Water Research 44(4):1082-1093
497   doi:https://doi.org/10.1016/j.watres.2009.09.027
498 Ma J, Ibekwe MA, Crowley DE, Yang C-H (2014) Persistence of *Escherichia coli* O157 and non-O157
499   strains in agricultural soils. The Science of the total environment 490:822-829
500   doi:http://dx.doi.org/10.1016/j.scitotenv.2014.05.069

501 Malvern (2014) Technical note: Measuring the zeta potential of high conductivity samples using the
502   Zetasizer Nano. In: Ltd MI (ed) UK.
503 Merritt JH, Kadouri DE, O'Toole GA (2011) Growing and analyzing static biofilms. Current Protocols in
504   Microbiology:00:B:1B.1:1B.1.1–1B.1.17 doi:10.1002/9780471729259.mc01b01s22
505 Moore BC, Martinez E, Gay JM, Rice DH (2003) Survival of *Salmonella enterica* in freshwater and
506   sediments and transmission by the aquatic midge *Chironomus tentans* (Chironomidae:
507   Diptera). Applied and environmental microbiology 69(8):4556-4560
508   doi:10.1128/aem.69.8.4556-4560.2003
509 Muirhead RW, Collins RP, Bremer PJ (2006a) The association of *E. coli* and soil particles in overland
510   flow. Water Science and Technology 54(3):153-9
511 Muirhead RW, Collins RP, Bremer PJ (2006b) Interaction of *Escherichia coli* and soil particles in
512   runoff. Applied and environmental microbiology 72(5):3406- 3411
513 Muirhead RW, Davies-Colley RJ, Donnison AM, Nagels JW (2004) Faecal bacteria yields in artificial
514   flood events: quantifying in-stream stores. Water Research 38(5):1215-24
515   doi:10.1016/j.watres.2003.12.010
516 O'Toole GA, Pratt LA, Watnick PI, Newman DK, Weaver VB, Kolter R (1999) Genetic approaches to
517   study of biofilms. Methods in Enzymology 310:91-109
518 Oliver DM, Clegg CD, Haygarth PM, Heathwaite AL (2005) Assessing the potential for pathogen
519   transfer from grassland soils to surface waters Advances in Agronomy. vol 85. Academic
520   Press, pp 125-180
521 Oliver DM, Clegg CD, Heathwaite AL, Haygarth PM (2007) Preferential attachment of *Escherichia coli*
522   to different particle size fractions of an agricultural grassland soil. Water, Air, and Soil
523   Pollution 185(1-4):369-375 doi:10.1007/s11270-007-9451-8
524 Pachepsky Y, Stocker M, Saldaña MO, Shelton D (2017) Enrichment of stream water with fecal
525   indicator organisms during baseflow periods. Environmental Monitoring and Assessment
526   189(2):51 doi:10.1007/s10661-016-5763-8
527 Pachepsky YA, Shelton DR (2011) *Escherichia coli* and fecal coliforms in freshwater and estuarine
528   sediments. Critical Reviews in Environmental Science and Technology 41(12):1067-1110
529   doi:10.1080/10643380903392718
530 Pachepsky YA, Yu O, Karns JS, Shelton DR, Guber AK, van Kessel JS (2008) Strain-dependent
531   variations in attachment of *E. coli* to soil particles of different sizes. International
532   Agrophysics 22:61-66
533 Perni S, Preedy EC, Prokopovich P (2014) Success and failure of colloidal approaches in adhesion of
534   microorganisms to surfaces. Advances in Colloid and Interface Science 206(Supplement
535   C):265-274 doi:https://doi.org/10.1016/j.cis.2013.11.008
536 Pond K (2005) Water recreation and disease. Plausibility of associated infections: acute effects,
537   sequelae and mortality. IWA Publishing in association with WHO, Geneva
538 Rijnaarts HHM, Norde W, Lyklema J, Zehnder AJB (1995) The isoelectric point of bacteria as an
539   indicator for the presence of cell surface polymers that inhibit adhesion. Colloids and
540   Surfaces B: Biointerfaces 4(4):191-197 doi:http://dx.doi.org/10.1016/0927-7765(94)01164-Z
541 Rong X, Huang Q, He X, Chen H, Cai P, Liang W (2008) Interaction of *Pseudomonas putida* with
542   kaolinite and montmorillonite: a combination study by equilibrium adsorption, ITC, SEM and
543   FTIR. Colloids and Surfaces B: Biointerfaces 64(1):49-55 doi:10.1016/j.colsurfb.2008.01.008
544 Roper MM, Marshall KC (1974) Modification of the interaction between *Escherichia coli* and
545   bacteriophage in saline sediment. Microbial Ecology 1(1- 13)
546 Rowe B, Gross RJ, Woodroof DP (1977) Proposal to recognise seroovar 145/46 (Synonyms: 147,
547   Shigella 13, *Shigella sofia*, and *Shigella manolovii*) as a new *Escherichia coli* 0 group, 0164.
548   International Journal of Systematic Bacteriology 27(1):15-18
549 SEPA (2013) River Ythan 2011-2013 database. SEPA (© Scottish Environment Protection Agency and
550   database right (2015) All rights reserved) (Accessed 2015)

551 Sevin DC, Stahlin JN, Pollak GR, Kuehne A, Sauer U (2016) Global Metabolic Responses to Salt Stress
552   in Fifteen Species. PloS one 11(2):e0148888 doi:10.1371/journal.pone.0148888
553 Sharma MM, Chang YI, Yen TF (1985) Reversible and irreversible surface charge modification of
554   bacteria for facilitating transport through porous media. Colloids and Surfaces 16:193-206
555 Shuval H (2003) Estimating the global burden of thalassogenic diseases: human infectious diseases
556   caused by wastewater pollution of the marine environment. Journal of water and health
557   1(2):53-64
558 Sokolov I, Smith DS, Henderson GS, Gorby YA, Ferris FG (2001) Cell surface electrochemical
559   heterogeneity of the Fe(III)-reducing bacteria *Shewanella putrefaciens*. Environmental
560   Science and Technology 35(2):341-347 doi:10.1021/es001258s
561 Van der Wal A, Minor M, Norde W, Zehnder AJB, Lyklema J (1997) Electrokinetic potential of
562   bacterial cells. Langmuir 13(2):165-171 doi:10.1021/la960386k
563 Van Loosdrecht MCM, Lyklema J, Norde W, Schraa G, Zehnder AJB (1987) Electrophoretic mobility
564   and hydrophobicity as a measure to predict the initial steps of bacterial adhesion. Applied
565   and environmental microbiology 53(8):1898- 1901
566 Van Loosdrecht MCM, Norde W, Lyklema J, Zehnder AB (1990) Hydrophobic and electrostatic
567   parameters in bacterial adhesion. Aquatic Sciences 52(1):103-114 doi:10.1007/bf00878244
568 Walker SL, Redman JA, Elimelech M (2004) Role of cell surface lipopolysaccharides in *Escherichia coli*
569   K12 adhesion and transport. Langmuir 20:7736- 7746
570 Whitehouse R (2000) Dynamics of estuarine muds: A manual for practical applications. Thomas
571   Telford
572 Wirth T, Falush D, Lan R, Colles F, Mensa P, Wieler LH, Karch H, Reeves PR, Maiden MCJ, Ochman H,
573   Achtman M (2006) Sex and virulence in *Escherichia coli*: an evolutionary perspective.
574   Molecular Microbiology 60(5):1136-1151 doi:10.1111/j.1365-2958.2006.05172.x
575 Wolfe AJ, Berg HC (1989) Migration of bacteria in semisolid agar. Proceedings of the National
576   Academy of Sciences of the United States of America 86(18):6973-7
577 Zhao W, Walker SL, Huang Q, Cai P (2014) Adhesion of bacterial pathogens to soil colloidal particles:
578   influences of cell type, natural organic matter, and solution chemistry. Water Research
579   53:35-46 doi:10.1016/j.watres.2014.01.009

580

| Strain	Serotype	Clade	MLST	Origin	Isolation	Details
Yth13	Unknown	B1	155	Ythan estuary, Scotland	2014	Isolated from a mixed mud sediment where salinity ~17 PSU.
DSM 8698	O111:H-	B1	20	DSMZ	1950	Enteropathogenic, isolated from human diarrhoea (Kauffmann and Dupont 1950)
DSM 9034	O164:H-	-	-	DSMZ	1947	Enteroinvasive, isolated from human diarrhoea (Rowe et al. 1977)

| Sediment Type	UK Grid Reference (Lat., Lon.)	Bulk Density (g cm^{-3} ± SE)	Water Content (% core weight ± SE)	Organic Content (% dry weight ± SE)	Surface Area (sq.m g^{-1})
Organic Mud	57.359746, -2.017193	1.27 ± 0.01	65.42 ± 0.12	9.12 ± 0.12	7.101
Mud	57.334826, -2.004501	1.38 ± 0.07	62.82 ± 0.26	7.00 ± 0.12	6.014
Mixed Sand	57.313898, -1.993890	1.95 ± 0.03	23.66 ± 0.17	2.16 ± 0.02	1.136

Strain	Biofilm (Relative adsorption at 600 nm ± SE)	Swarm Diameter (mm ± SE)						
		15 ˚C Day 3	15 ˚C Day 5	15 ˚C Day 10	15 ˚C Day 15	25 ˚C Day 1	25 ˚C Day 3	25 ˚C Day 6
Yth13	0.129 ± 0.029	7.00 ± 0.00	9.00 ± 0.00	12.67 ± 0.33	16.67 ± 0.67	5.00 ± 0.00	10.67 ± 0.33	17.33 ± 0.33
DSM 8698	0.546 ± 0.080	5.67 ± 0.33	7.00 ± 0.00	11.00 ± 0.58	13.00 ± 0.58	39.33 ± 11.68	> 85.00	> 85.00
DSM 9034	0.033 ± 0.012	4.00 ± 0.00	4.67 ± 0.33	5.33 ± 0.67	6.00 ± 1.15	4.00 ± 0.00	7.67 ± 0.33	10.33 ± 0.67

Sediment	Organic Mud	Mud	Mixed Sand		F- statistic	p- value
Mean ($\log_{10}$ CFU ml^{-1} ± SE)	0.334 ± 0.020	0.299 ± 0.034	0.272 ± 0.029		5.34	0.007 (OM > MS)

Strain	Yth13	DSM 8698	DSM 9034		F- statistic	p- value
Mean ($\log_{10}$ CFU ml^{-1} ± SE)	0.265 ± 0.027	0.403 ± 0.030	0.238 ± 0.019		43.38	<0.001 (DSM 8698 > DSM 9034, Yth13)

Salinity (PSU)	0	2	3.5	5	F- statistic	p- value
Mean ($\log_{10}$ CFU ml^{-1} ± SE)	0.243 ± 0.020	0.350 ± 0.044	0.361 ± 0.031	0.254 ± 0.026	15.87	<0.001 (2, 3.5 > 0, 5)

		Strain			Salinity (PSU)			
		Yth13	DSM 8698	DSM 9034	0	2	3.5	5
Sediment	**Organic Mud**	0.356 ± 0.043	0.323 ± 0.042	0.323 ± 0.015	0.289 ± 0.021	0.356 ± 0.047	0.410 ± 0.051	0.281 ± 0.024
	Mud	0.272 ± 0.036	0.512 ± 0.047	0.114 ± 0.019	0.226 ± 0.040	0.341 ± 0.105	0.354 ± 0.061	0.276 ± 0.054
	Mixed Sand	0.166 ± 0.047	0.374 ± 0.053	0.275 ± 0.029	0.213 ± 0.037	0.350 ± 0.075	0.321 ± 0.051	0.204 ± 0.052
Salinity (PSU)	**0**	0.219 ± 0.024	0.251 ± 0.040	0.258 ± 0.039				
	2	0.198 ± 0.024	0.627 ± 0.043	0.223 ± 0.043				
	3.5	0.474 ± 0.049	0.379 ± 0.030	0.231 ± 0.050				
	5	0.168 ± 0.044	0.356 ± 0.042	0.238 ± 0.025				
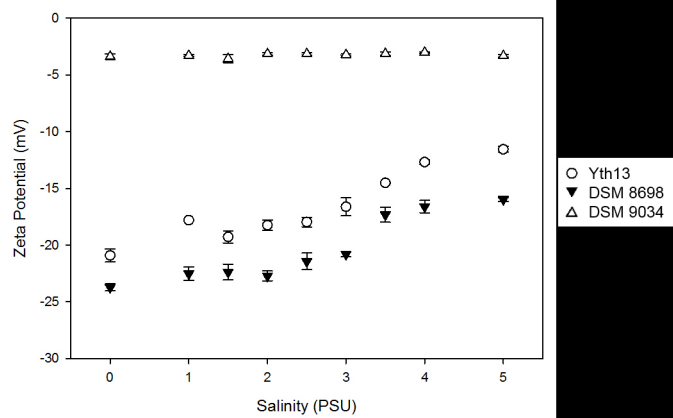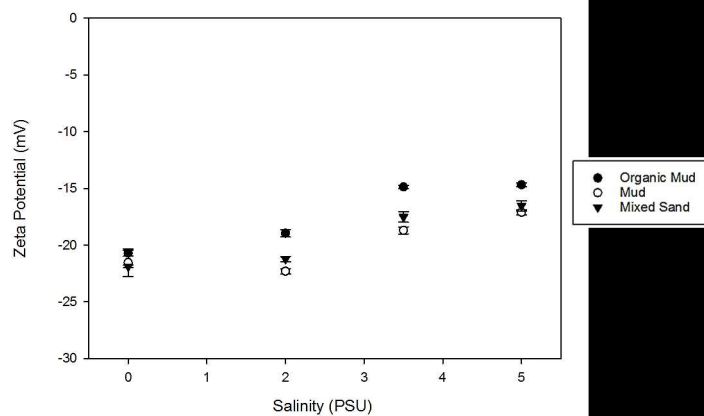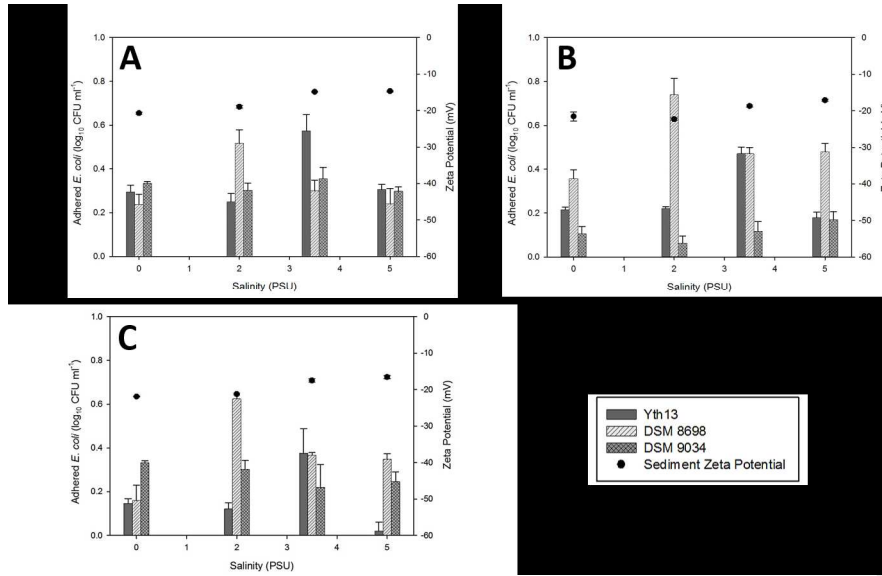
Highlights

- *E. coli* zeta potential profiles differ between strains over a salinity gradient

- Adhesion efficiency depended on strain > salinity > sediment

- Zeta potential did not influence adhesion efficiency

- Adhesion to sediments was greatest at moderate salinities tested (2 and 3.5 PSU)